Static analysis and design of revolute joint and antiparallelogram joint: a technical report

Vimalesh Muralidharan

Static analysis and design of revolute joint and antiparallelogram joint: a technical report

Vimalesh Muralidharan

Abstract

This technical report details the derivation of the static models of two antagonistically actuated joints: revolute (R) joint and antiparallelogram (X) joint. The conditions for these joints to possess the specified wrench-feasible workspace with the prescribed stiffness are derived. Using these conditions as constraints, a strategy for the optimal design of these joints is proposed that with an objective of minimizing the forces required to move them.

1 Organisation of the report

Two antagonistically actuated joints namely, the revolute joint or the R-joint and the antiparallelogram joint, also referred to as the X-joint, are studied in this report. The analysis of the R-joint is carried out in Section 2, and the X-joint in Section 3. The organization of each of these sections are identical and are detailed in the following. Firstly, a generalized coordinate is identified to describe the configuration of the joint, and all the dependent coordinates are obtained in terms of this coordinate for further study. This is followed by static analysis of the joint, where the expression of total potential energy is derived, followed by the equation of static equilibrium and stiffness. Following this, an optimisation problem for the design of these joints are posed and solved in Section 4. Finally, the conclusion of this study is presented in Section 5.

2 R-joint

A schematic of the R-joint is shown in Fig. 1. It consists of two congruent isosceles triangles, one on top of another, connected by a revolute joint at point $\boldsymbol{o}$. The joint is equipped with two identical springs (spring constant, k) on either side to impart stiffness into the system. It is actuated by two cables passing through the middle of the springs, by applying forces, F_1 and F_2, respectively. Additionally, a point mass M is attached to the segment $\boldsymbol{p}_1\boldsymbol{p}_2$ at a distance d. The linear mass density (i.e., mass per unit length) of the links is given by ρ.

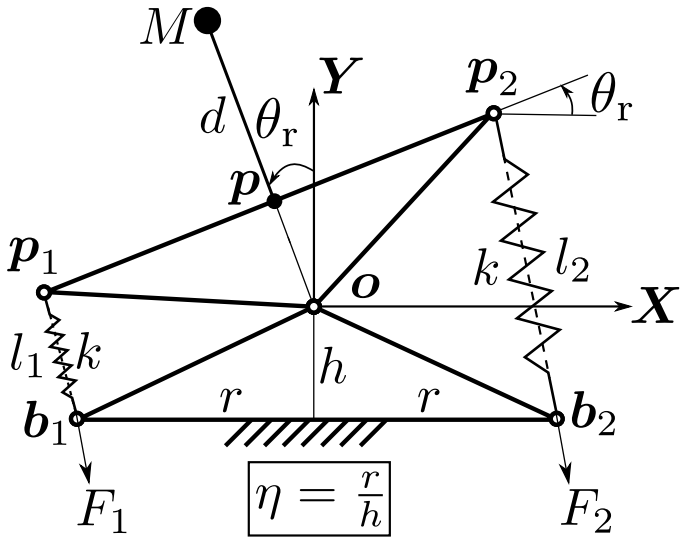

Figure 1: Schematic of the pivot joint.

The generalized coordinate that describes the configuration of the joint is considered to be θ_r. The dependent coordinates l_1 and l_2 are expressed as a function of θ_r, for further use in the upcoming sections. The following relations can be obtained using elementary geometric principles:

$$l_1 = 2\left(h\cos\frac{\theta_r}{2} - r\sin\frac{\theta_r}{2}\right); \quad l_2 = 2\left(h\cos\frac{\theta_r}{2} + r\sin\frac{\theta_r}{2}\right). \tag{1}$$

The derivatives of l_1, l_2 w.r.t. θ_r are:

$$\frac{\mathrm{d}l_1}{\mathrm{d}\theta_r} = -\left(h\sin\frac{\theta_r}{2} + r\cos\frac{\theta_r}{2}\right); \quad \frac{\mathrm{d}l_2}{\mathrm{d}\theta_r} = \left(-h\sin\frac{\theta_r}{2} + r\cos\frac{\theta_r}{2}\right); \tag{2}$$

$$\frac{\mathrm{d}^2l_1}{\mathrm{d}\theta_r^2} = \frac{1}{2}\left(-h\cos\frac{\theta_r}{2} + r\sin\frac{\theta_r}{2}\right); \quad \frac{\mathrm{d}^2l_2}{\mathrm{d}\theta_r^2} = -\frac{1}{2}\left(h\cos\frac{\theta_r}{2} + r\sin\frac{\theta_r}{2}\right). \tag{3}$$

2.1 Limits of motion of the R-joint due to singularities

The direction of the applied forces F_1 and F_2 are not defined when $l_1 = 0$ and $l_2 = 0$, respectively. Hence, it is not possible to control the manipulator in these configurations, and consequently, they define the boundaries of the wrench-feasible workspace (when no limits are imposed on the forces applied by the tendons) of the module. This is illustrated in Fig. 2.

Cable-driven manipulators also suffer from force-closure singularities in addition to the singularities observed in parallel manipulators. Force-closure singularities refer to the configurations where the manipulator cannot withstand an arbitrary external wrench applied on one of the links, when all the cables are in tension and locked. For the pivot module, such situations occur when the line of action of force, l_1 or l_2 passes through the point $\boldsymbol{o}$ as illustrated in Fig. 3.

However, the limits of motion are defined by only one of these singularities, depending on the ratio $\frac{r}{h}$. From the Figs. 2 and 3, the following observations on the limits of motion can be made:

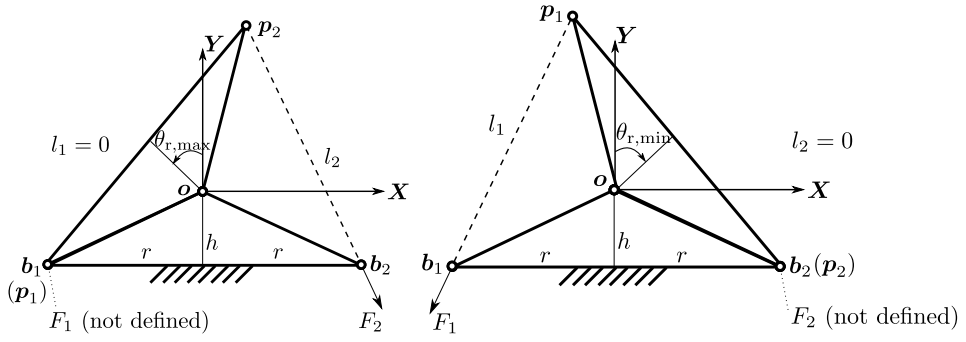

(a) Singularity for the first cable (b) Singularity for the second cable

Figure 2: Limits of motion for the R-joint due to the vanishing of l_1 and l_2.

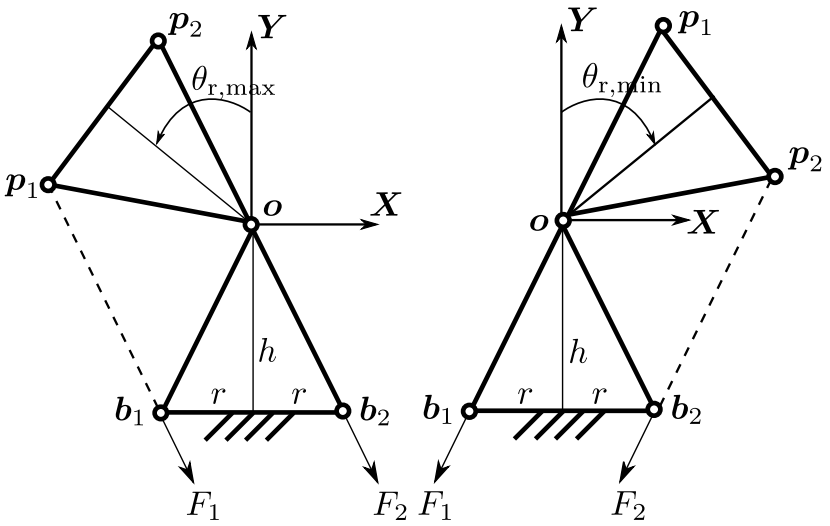

(a) Singularity for the second cable (b) Singularity for the first cable

Figure 3: Limits of motion for the R-joint due to force-closure singularity.

- Case 1 ($r > h$): The limit of motion is formed by $l_i = 0, i = 1, 2$, leading to: $\theta_\mathrm{r} \in (-\left(\pi - 2\tan^{-1}\left(\frac{r}{h}\right)\right), \left(\pi - 2\tan^{-1}\left(\frac{r}{h}\right)\right)$.
- Case 2 ($r < h$): Occurrence of force-closure singularity limits the motion, leading to: $\theta_\mathrm{r} \in \left(-2\tan^{-1}\left(\frac{r}{h}\right), 2\tan^{-1}\left(\frac{r}{h}\right)\right)$
- Case 3 ($r = h$): Limit of motion is formed by both $l_i = 0, i = 1, 2$ and force-closure singularity simultaneously: $\theta_\mathrm{r} \in \left(-\frac{\pi}{2}, \frac{\pi}{2}\right)$

2.2 Static analysis of the R-joint

The expression of total potential energy of the joint is obtained as the sum of potential due to gravity (U_g), springs (U_sp), and external forces applied by the tendons (U_f):

$$U_\mathrm{r} = U_\mathrm{g} + U_\mathrm{sp} + U_\mathrm{f}, \tag{4}$$

$$U_\mathrm{r} = \frac{4}{3}\rho g h(r + \sqrt{r^2 + h^2})\cos\theta_\mathrm{r} + Mg(d + h)\cos\theta_\mathrm{r} + 2k\left(r^2 + h^2 - \left(r^2 - h^2\right)\cos\theta_\mathrm{r}\right) + F_1 l_1 + F_2 l_2, \tag{5}$$

Differentiation of this expression w.r.t. θ_r leads to the equation of static equilibrium, which is of the form: $G_\mathrm{r} = \Gamma_\mathrm{r}$, where:

$$G_\mathrm{r} = C\sin\theta_\mathrm{r}, \text{ with } C = \frac{1}{3}\left(6k\left(r^2 - h^2\right) - 4\rho g h(r + \sqrt{r^2 + h^2}) - 3Mg\left(d + h\right)\right); \tag{6}$$

$$\Gamma_\mathrm{r} = -F_1\frac{\mathrm{d}l_1}{\mathrm{d}\theta_\mathrm{r}} - F_2\frac{\mathrm{d}l_2}{\mathrm{d}\theta_\mathrm{r}} = F_1\left(h\sin\frac{\theta_\mathrm{r}}{2} + r\cos\frac{\theta_\mathrm{r}}{2}\right) + F_2\left(h\sin\frac{\theta_\mathrm{r}}{2} - r\cos\frac{\theta_\mathrm{r}}{2}\right). \tag{7}$$

The symbol G_r represents the wrench due to gravity and the springs, while Γ_r represents the external wrench that can be provided by the tendons. From Eq. (1), it can be shown that the coefficients of F_1 and F_2 are positive and negative, respectively, within the limits of motion in all the cases listed in Section 2.1. This result is also intuitive from Fig. 1, as it is apparent that F_1 applies an anticlockwise moment, and F_2 a clockwise moment on the joint, respectively.

Also, the forces provided by the cables are limited physically, leading to: $F_1, F_2 \in [F_\mathrm{min}, F_\mathrm{max}]$. Since the coefficient of F_1 (resp. F_2) in Γ_r is always negative (resp. positive), the maximal (resp. minimal) boundary of the available wrench Γ_max (resp. Γ_min) is obtained when $F_1 = F_\mathrm{max}$ and $F_2 = F_\mathrm{min}$ (resp. $F_1 = F_\mathrm{min}$ and $F_2 = F_\mathrm{max}$). Considering these limits on Γ_r, it follows that the equation of static equilibrium can be satisfied only when: $G_\mathrm{r} \in [\Gamma_\mathrm{min}, \Gamma_\mathrm{max}]$.

The expression of stiffness of the module is obtained by considering the second derivative of the total potential function w.r.t. θ_r as follows:

$$K_\mathrm{r} = C\cos\theta_\mathrm{r} + \frac{1}{2}F_1\left(-h\cos\frac{\theta_\mathrm{r}}{2} + r\sin\frac{\theta_\mathrm{r}}{2}\right) - \frac{1}{2}F_2\left(h\cos\frac{\theta_\mathrm{r}}{2} + r\sin\frac{\theta_\mathrm{r}}{2}\right). \tag{8}$$

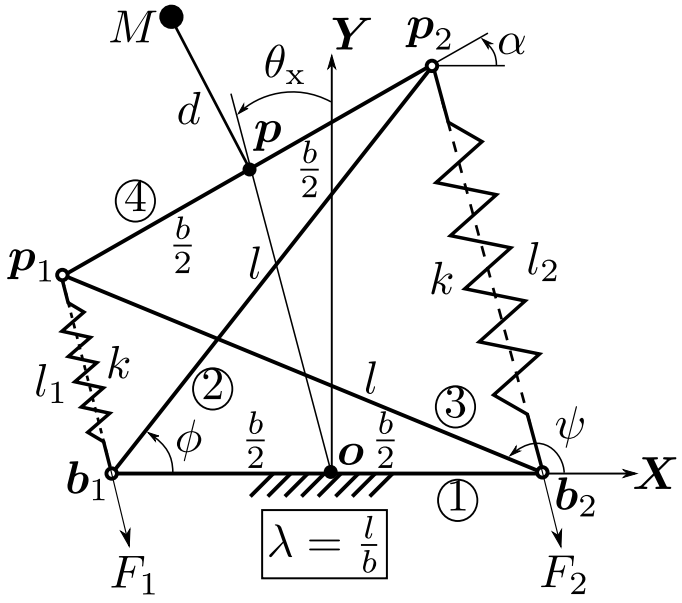

Figure 4: Schematic of the X-joint.

3 X-joint

The schematic of the X-joint is shown in Fig. 4. It contains three moving links $2, 3, 4$ and one fixed link 1. The top and bottom bars $(1, 4)$ are of length b, while the crossed bars $(2, 3)$ are of length b. It is noted that the condition, $l > b$ must be satisfied for the assembly of the joint. The other parameters k, ρ, M, d, F_1, F_2 possess the same definitions as in the case of the R-joint (see Section 2).

The configuration of the X-joint is denoted by the orientation angle (θ_x) of the segment connecting the midpoints of the bars 1 and 4 w.r.t. the vertical (see Fig. 4). All the other dependent coordinates can be expressed as a function of θ_x, using elementary geometric principles, as follows:

$$
\begin{aligned}
&\alpha = 2\theta_x;\\
&\cos\phi = \frac{\left(b\cos^2\theta_x - \sin\theta_x\sqrt{l^2 - b^2\cos^2\theta_x}\right)}{l}; \quad \sin\phi = \frac{\left(b\sin\theta_x + \sqrt{l^2 - b^2\cos^2\theta_x}\right)}{l};\\
&\cos\psi = -\frac{\left(b\cos^2\theta_x + \sin\theta_x\sqrt{l^2 - b^2\cos^2\theta_x}\right)}{l}; \quad \sin\psi = \frac{\left(-b\sin\theta_x + \sqrt{l^2 - b^2\cos^2\theta_x}\right)}{l};\\
&l_1 = -b\sin\theta_x + \sqrt{l^2 - b^2\cos^2\theta_x}; \quad l_2 = b\sin\theta_x + \sqrt{l^2 - b^2\cos^2\theta_x}.
\end{aligned}
\tag{9}
$$

Differentiation of l_1 and l_2 w.r.t. θ_x yields:

$$
\frac{\mathrm{d}l_1}{\mathrm{d}\theta_x} = b\cos\theta_x\left(\frac{b\sin\theta_x}{\sqrt{l^2 - b^2\cos^2\theta_x}} - 1\right); \quad \frac{\mathrm{d}l_2}{\mathrm{d}\theta_x} = b\cos\theta_x\left(\frac{b\sin\theta_x}{\sqrt{l^2 - b^2\cos^2\theta_x}} + 1\right). \tag{10}
$$

Further differentiation w.r.t. θ_x results in:

$$
\frac{\mathrm{d}^2l_1}{\mathrm{d}\theta_x^2} = b\left(\frac{bl^2\cos 2\theta_x - b^3\cos^4\theta_x}{\left(l^2 - b^2\cos^2\theta_x\right)^{3/2}} + \sin\theta_x\right); \quad \frac{\mathrm{d}^2l_2}{\mathrm{d}\theta_x^2} = b\left(\frac{bl^2\cos 2\theta_x - b^3\cos^4\theta_x}{\left(\lambda^2 - b^2\cos^2\theta_x\right)^{3/2}} - \sin\theta_x\right). \tag{11}
$$

Unlike the R-joint, the motion of the X-joint is always limited by the occurrence of parallel singularities at $\theta_{\mathrm{x}} = \pm\frac{\pi}{2}$, irrespective of the dimensions of the links.

3.1 Static analysis of the X-joint

The expression for total potential energy of the X-joint is obtained in a manner similar to that of the pivot joint, as:

$$U_{\mathrm{x}} = -\cos 2\theta_{\mathrm{x}} \left(b^2 k - dgM\right) + (\rho(b+l) + M)g\cos\theta_{\mathrm{x}}\sqrt{l^2 - b^2\cos^2\theta_{\mathrm{x}}} + kl^2 + F_1 l_1 + F_2 l_2; \quad (12)$$

Differentiating the total potential energy w.r.t. θ_{x} leads to the equation of static equilibrium: $G_{\mathrm{x}} = \Gamma_{\mathrm{x}}$, with:

$$G_{\mathrm{x}} = C_1 \sin 2\theta_{\mathrm{x}} + \frac{C_2 \sin\theta_{\mathrm{x}}\left(2b^2\cos^2\theta_{\mathrm{x}} - l^2\right)}{b\sqrt{l^2 - b^2\cos^2\theta_{\mathrm{x}}}}; \text{ where } C_1 = 2(b^2 k - Mgd), C_2 = bg(M + \rho(b+l)); \quad (13)$$

$$\Gamma_{\mathrm{x}} = -F_1\frac{\mathrm{d}l_1}{\mathrm{d}\theta_{\mathrm{x}}} - F_2\frac{\mathrm{d}l_2}{\mathrm{d}\theta_{\mathrm{x}}} = F_1 b\cos\theta_{\mathrm{x}}\left(\frac{\sqrt{l^2 - b^2\cos^2\theta_{\mathrm{x}}} - b\sin\theta_{\mathrm{x}}}{\sqrt{l^2 - b^2\cos^2\theta_{\mathrm{x}}}}\right) - F_2 b\cos\theta_{\mathrm{x}}\left(\frac{\sqrt{l^2 - b^2\cos^2\theta_{\mathrm{x}}} + b\sin\theta_{\mathrm{x}}}{\sqrt{l^2 - b^2\cos^2\theta_{\mathrm{x}}}}\right), \quad (14)$$

The symbols G_{x} and Γ_{x} possess the same physical meaning as in case of the pivot joint. It can be shown that the coefficient of F_1 in the expression of Γ_{x}, is positive from the assembly condition $l > b$ and the following argument: $b\sqrt{\frac{l^2}{b^2} - \cos^2\theta_{\mathrm{x}}} > \sin\theta_{\mathrm{x}} (= b\sqrt{1 - \cos^2\theta_{\mathrm{x}}})$. Also, from Eq. (14), it is clear that the coefficient of F_2 is negative. This shows that the upper bound Γ_{x} occurs when $F_1 = F_{\max}, F_2 = F_{\min}$ and the lower bound occurs when $F_1 = F_{\min}, F_2 = F_{\max}$.

The expression of stiffness of the module is obtained by computing the second derivative of the total potential function w.r.t. θ_{x} as follows:

$$\begin{aligned} K_{\mathrm{x}} =& \frac{\mathrm{d}(G-\Gamma)}{\mathrm{d}\theta_{\mathrm{x}}} = \frac{\mathrm{d}G}{\mathrm{d}\theta_{\mathrm{x}}} + F_1\frac{\mathrm{d}^2 l_1}{\mathrm{d}\theta_{\mathrm{x}}^2} + F_2\frac{\mathrm{d}^2 l_2}{\mathrm{d}\theta_{\mathrm{x}}^2} \\ =& 2C_1\cos 2\theta_{\mathrm{x}} - \frac{C_2\cos\theta_{\mathrm{x}}\left(\left(l^2 - b^2\cos 2\theta_{\mathrm{x}}\right)^2 - b^2\left(l^2 - b^2\right)\cos 2\theta_{\mathrm{x}}\right)}{b\left(l^2 - b^2\cos^2\theta_{\mathrm{x}}\right)^{3/2}} \quad (15) \\ &+ bF_1\left(\frac{bl^2\cos 2\theta_{\mathrm{x}} - b^3\cos^4\theta_{\mathrm{x}}}{\left(l^2 - b^2\cos^2\theta_{\mathrm{x}}\right)^{3/2}} + \sin\theta_{\mathrm{x}}\right) + bF_2\left(\frac{bl^2\cos 2\theta_{\mathrm{x}} - b^3\cos^4\theta_{\mathrm{x}}}{\left(\lambda^2 - b^2\cos^2\theta_{\mathrm{x}}\right)^{3/2}} - \sin\theta_{\mathrm{x}}\right) \quad (16) \end{aligned}$$

4 Optimal design of the joints

In this study, the link lengths and the spring constant of the joints are considered to be the design variables, while the linear mass density and payload characteristics (ρ, M, d) are treated as parameters whose values are known *a priori*. The goal is to find optimal designs of the joints, such that the following conditions are met:

- The joint should possess the specified WFW of the general form: $[-\theta_{\max}, \theta_{\max}]$ with $\theta_{\max} < \frac{\pi}{2}$ to avoid singularities.
- The joint stiffness must be non-negative throughout the WFW for all admissible values of forces satisfying the equation of static equilibrium. Additionally, the stiffness must be equal to a prescribed value ($K_0 > 0$) when no actuation forces (F_1, F_2) are applied and equal to ($K_1 > 0$) at the boundary of the WFW.
- The force required to move the joint must be a minimum.

Due to symmetry of the joints about their respective zero orientations, ensuring $[0, \theta_{\max}] \in$ WFW, ensures that $[-\theta_{\max}, 0] \in$ WFW. Similar arguments can be made about the non-negativeness of the stiffness of the joints as well. This makes it sufficient to study just one half of the problem, i.e., $\theta_{\mathrm{r}} > 0$ and $\theta_{\mathrm{x}} > 0$. In the following, the positive boundary of WFW is denoted by θ_{rm} for the R-joint, and θ_{xm} for the X-joint. In order to satisfy the conditions listed above, a system of equations and inequalities have been formulated for the two joints as shown in Table 1 (assuming $F_{\min} = 0$). Physically, the first two conditions ensure that no singularities occur within the WFW and that the positive boundary of the WFW is formed by the intersection of the curves G_{r} (resp. G_{x}) and $\Gamma_{\max}$. The third and fifth conditions ensure that the stiffness of the joint is equal to K_0 in the

Table 1: Formulation of the stipulated conditions for the R-joint and the X-joint.

R-joint		X-joint	
$l_1(\theta_{\mathrm{rm}}) > 0$	(17a)	No singularities when $\left(\theta_{\mathrm{xm}} < \dfrac{\pi}{2}\right)$	(18a)
$G_{\mathrm{r}}(\theta_{\mathrm{rm}}) + F_{\max}\dfrac{\mathrm{d}l_1}{\mathrm{d}\theta_{\mathrm{r}}}(\theta_{\mathrm{rm}}) = 0$	(17b)	$G_{\mathrm{x}}(\theta_{\mathrm{xm}}) + F_{\max}\dfrac{\mathrm{d}l_1}{\mathrm{d}\theta_{\mathrm{x}}}(\theta_{\mathrm{xm}}) = 0$	(18b)
$K_{\mathrm{r}}(\theta_{\mathrm{r}} = 0, F_1 = 0, F_2 = 0) = K_0$	(17c)	$K_{\mathrm{x}}(\theta_{\mathrm{x}} = 0, F_1 = 0, F_2 = 0) = K_0$	(18c)
$K_{\mathrm{r}}(\theta_{\mathrm{r}} = 0, F_1 = F_{\max}, F_2 = F_{\max}) \geq 0$	(17d)	$K_{\mathrm{x}}(\theta_{\mathrm{x}} = 0, F_1 = F_{\max}, F_2 = F_{\max}) \geq 0$	(18d)
$K_{\mathrm{r}}(\theta_{\mathrm{r}} = \theta_{\mathrm{rm}}, F_1 = F_{\max}, F_2 = 0) = K_1$	(17e)	$K_{\mathrm{x}}(\theta_{\mathrm{x}} = \theta_{\mathrm{xm}}, F_1 = F_{\max}, F_2 = 0) = K_1$	(18e)

absence of applied forces, and equal to K_1 at the boundary of the WFW. The remaining condition ensures that the joint possesses a non-negative stiffness at the zero orientation when maximum forces are applied. The ratio of link lengths: $\eta(= \frac{r}{h})$ for the R-joint and $\lambda(= \frac{l}{b})$ for the X-joint have been introduced into the formulation, eliminating the variables h and l, respectively. This is because the ratio provides more insights into the problem and also simplifies the resulting expressions considerably. The conditions in Table 1 are then derived in terms of the joint parameters in the Sections 4.1 and 4.2. Using these expressions, design optimization problems for the R-joint and the X-joint are formulated and solved in the following.

4.1 Optimal design of the R-joint

It is noted that the set of design variables of the R-joint is formed by r, η, and k. From Eq. (17a) following condition is obtained:

$$\eta < \cot \frac{\theta_{\mathrm{rm}}}{2} \tag{19}$$

Equation (17c) yields:

$$C = K_0 \tag{20}$$

Substituting the expression of C from Eq. (6) into the above equation and solving for k results in:

$$k = \frac{\eta^2}{2r^2\left(\eta^2 - 1\right)} \left(K_0 + \frac{4r^2}{3\eta^2} \rho g \left(\eta + \sqrt{\eta^2 + 1} \right) + Mg \left(d + \frac{r}{\eta} \right) \right) \tag{21}$$

From the above equation, it is clear the condition $\eta > 1$ is necessary to ensure that k remains positive. Equation (17b) leads to:

$$-C \sin \theta_{\mathrm{rm}} + \frac{r}{\eta} F_{\max} \sin \frac{\theta_{\mathrm{rm}}}{2} + F_{\max} r \cos \frac{\theta_{\mathrm{rm}}}{2} = 0 \tag{22}$$

Substituting for C from Eq. (20) into Eq. (22) and solving for $F_{\max}$ yields:

$$F_{\max} = \frac{K_0 \eta \sin \theta_{\mathrm{rm}}}{r\left(\eta \cos \frac{\theta_{\mathrm{rm}}}{2} + \sin \frac{\theta_{\mathrm{rm}}}{2} \right)} \tag{23}$$

From Eq. (17e), one obtains:

$$C \cos \theta_{\mathrm{rm}} + \frac{1}{2} F_{\max} r \sin \frac{\theta_{\mathrm{rm}}}{2} - \frac{r \cos \frac{\theta_{\mathrm{rm}}}{2}}{\eta} - K_1 = 0 \tag{24}$$

Upon substitution of the expressions for C and $F_{\max}$ from Eq. (20) and (23) into the Eq. (24):

$$\frac{K_0 \sin \theta_{\mathrm{rm}} \left(\eta \sin \frac{\theta_{\mathrm{rm}}}{2} - \cos \frac{\theta_{\mathrm{rm}}}{2} \right)}{2\left(\eta \cos \frac{\theta_{\mathrm{rm}}}{2} + \sin \frac{\theta_{\mathrm{rm}}}{2} \right)} + K_0 \cos \theta_{\mathrm{rm}} - K_1 = 0 \tag{25}$$

Solving for η from the above equation, results in:

$$\eta = \frac{K_0(1 - \cos \theta_{\mathrm{rm}}) + 2K_1}{K_0(1 + \cos \theta_{\mathrm{rm}}) - 2K_1} \tan \frac{\theta_{\mathrm{rm}}}{2} \tag{26}$$

The above equation provides a simple relationship between the design specifications $(\theta_{\mathrm{rm}}, K_0, K_1)$ and η. This is quite interesting because for a given set of specifications, the ratio of link dimensions remains fixed, irrespective of the payload (M, d) and the material of the links (ρ). It is noted that the specifications K_0, K_1, and θ_{rm}, must allow the bounds on: $\eta \in]1, \cot \frac{\theta_{\mathrm{rm}}}{2}[$ to be satisfied, for the existence of feasible designs. By substituting the expression of η from Eq. (26) into Eqs. (21)

and (23), it is possible to find k and $F_{\max}$ solely in terms of r, the only design variable left in this problem.

The inequality in Eq. (17d), results in:

$$C - F_{\max}\frac{r}{\eta} \geq 0 \tag{27}$$

Substituting the the conditions in Eqs. (20) and (23), leads to:

$$\eta \geq \tan\frac{\theta_{\rm rm}}{2}\left(2\cos\frac{\theta_{\rm rm}}{2} - 1\right) \tag{28}$$

Given that $\theta_{\rm rm} \in]0, \frac{\pi}{2}[$, it is apparent that right hand side of the above inequality would always be less than 1. But, from Eq. (21), it has been shown that $\eta > 1$ is a necessary condition for k to be positive. Thus, the inequality in Eq. (28) remains satisfied by default without any imposing any additional conditions.

Hence, an optimization problem for the minimization of applied force may be posed as follows:

$$\begin{aligned} \underset{r}{\text{Minimize}} \quad & F_{\max}(r) = \frac{K_0(1-\cos\theta_{\rm rm}) + 2K_1}{r}\sin\frac{\theta_{\rm rm}}{2} \\ \text{subject to} \quad & r \in [0.025, 0.1]\,, \\ & k \in [0, 2000]\,, \end{aligned} \tag{29}$$

where r is the design variable of this problem. The constraint on η is not mentioned in the problem as it should be satisfied by the choice of K_0, K_1, and $\theta_{\rm rm}$. Bounds on the variables r and k have been imposed in the problem due to practical considerations, such as, availability of corresponding components in the market and ease of fabrication/assembly. Using Eq. (21), equivalent algebraic conditions on r, corresponding to bounds on k can be obtained. For instance, the condition $k \leq k_{\max}(= 2000)$ leads to a quadratic expression in r that must be non-negative:

$$\left(6\left(\eta^2-1\right)k_{\max} - 4g\left(\sqrt{\eta^2+1}+\eta\right)\rho\right)r^2 - 3Mg\eta r - 3\left(Mbd\eta^2 + \eta^2 K_0\right) \geq 0 \tag{30}$$

It is noted that the expression of η is known from Eq. (26), but it has not been substituted, to keep the resulting expressions short. In the limiting case when the inequality in Eq. (30) becomes an equality, the solutions for r can be found analytically as follows:

$$r_1 = \frac{3g\eta M - \sqrt{9g^2\eta^2M^2 - 4\left(6\left(\eta^2-1\right)k_{\max} - 4g\left(\sqrt{\eta^2+1}+\eta\right)\rho\right)\left(-3dg\eta^2M - 3\eta^2K_0\right)}}{2\left(6\left(\eta^2-1\right)k_{\max} - 4g\left(\sqrt{\eta^2+1}+\eta\right)\rho\right)}, \tag{31}$$

$$r_2 = \frac{3g\eta M + \sqrt{9g^2\eta^2M^2 - 4\left(6\left(\eta^2-1\right)k_{\max} - 4g\left(\sqrt{\eta^2+1}+\eta\right)\rho\right)\left(-3dg\eta^2M - 3\eta^2K_0\right)}}{2\left(6\left(\eta^2-1\right)k_{\max} - 4g\left(\sqrt{\eta^2+1}+\eta\right)\rho\right)} \tag{32}$$

The feasible range of r corresponding to the inequality in Eq. (30) will reduce the design space to $r \in [r_1, r_2]$ or $r \in (-\infty, r_1)\bigcup(\infty, r_2)$, depending upon the values assigned to the parameters in

the problem. These conditions would be used for defining the feasible design space of the R-joint. Similar constraints would be defined for the constraint: $k \geq k_{\min}$, as well.

The first-order necessary condition for $F_{\max}$ to achieve a local minima requires the vanishing of its derivative w.r.t. r. However, it is found that $\frac{\mathrm{d}F_{\max}}{\mathrm{d}r} = -\frac{K_0(1-\cos\theta_{\mathrm{rm}})+2K_1}{r^2}\sin\left(\frac{\theta_{\mathrm{rm}}}{2}\right)$, is negative for all feasible values of the design variables and parameters. This implies that $F_{\max}$ decreases with increase in r, and its minimum value would occur when r is as large as possible, while satisfying the constraints specified in Eq. (29). Further information on the minimum value of force and the corresponding design variables can be obtained by studying the behavior of $F_{\max}$ inside the design space with numerical values for the parameters.

4.2 Optimal design of the X-joint

It is noted that the set of design variables of the X-joint is formed by: b, λ, and k. Equation (18b) results in:

$$bF_{\max}\cos\theta_{\mathrm{xm}}\left(\frac{\sin\theta_{\mathrm{xm}}}{\sqrt{\lambda^2-\cos^2\theta_{\mathrm{xm}}}}-1\right)+C_1\sin 2\theta_{\mathrm{xm}}+\frac{C_2\sin\theta_{\mathrm{xm}}\left(2\cos^2\theta_{\mathrm{xm}}-\lambda^2\right)}{\sqrt{\lambda^2-\cos^2\theta_{\mathrm{xm}}}}=0 \tag{33}$$

Equation (18e) leads to:

$$\begin{aligned} bF_{\max}\left(\frac{\lambda^2\cos 2\theta_{\mathrm{xm}}-\cos^4\theta_{\mathrm{xm}}}{\left(\lambda^2-\cos^2\theta_{\mathrm{xm}}\right)^{3/2}}+\sin\theta_{\mathrm{xm}}\right)+2C_1\cos 2\theta_{\mathrm{xm}}-K_1 \\ -\frac{C_2\cos\theta_{\mathrm{xm}}\left(\left(\lambda^2-\cos 2\theta_{\mathrm{xm}}\right)^2-\left(\lambda^2-1\right)\cos 2\theta_{\mathrm{xm}}\right)}{\left(\lambda^2-\cos^2\theta_{\mathrm{xm}}\right)^{3/2}}=0 \end{aligned} \tag{34}$$

From Eq. (33) and (34), it is possible to solve for $F_{\max}$ and C_1 as follows:

$$F_{\max}=\frac{\left(C_2\lambda^4\sin\theta_{\mathrm{xm}}\tan^2\theta_{\mathrm{xm}}+K_1\tan\theta_{\mathrm{xm}}\left(\lambda^2-\cos^2\theta_{\mathrm{xm}}\right)^{3/2}\right)}{b\cos\theta_{\mathrm{xm}}\left(\left(\lambda^2-\cos^2\theta_{\mathrm{xm}}\right)^{3/2}-\sin^3\theta_{\mathrm{xm}}\right)} \tag{35}$$

$$C_1=\gamma_1K_1+\gamma_2C_2 \tag{36}$$

where

$$\gamma_1=\frac{\sec^2\theta_{\mathrm{xm}}\left(\lambda^2-\cos^2\theta_{\mathrm{xm}}\right)}{2\left(\sin\theta_{\mathrm{xm}}\sqrt{\lambda^2-\cos^2\theta_{\mathrm{xm}}}+\sin^2\theta_{\mathrm{xm}}-\cos^2\theta_{\mathrm{xm}}+\lambda^2\right)} \tag{37}$$

$$\begin{aligned} \gamma_2=\Bigg(&\lambda^4\sec^3\theta_{\mathrm{xm}}-\cos\theta_{\mathrm{xm}}\left(\sin\theta_{\mathrm{xm}}\sqrt{\lambda^2-\cos^2\theta_{\mathrm{xm}}}+2\sin^2\theta_{\mathrm{xm}}+3\lambda^2\right)\\ &+\tan\theta_{\mathrm{xm}}\left(\lambda^2\sin\theta_{\mathrm{xm}}+\left(\lambda^2-1\right)\sqrt{\lambda^2-\cos^2\theta_{\mathrm{xm}}}+\sin^2\theta_{\mathrm{xm}}\sqrt{\lambda^2-\cos^2\theta_{\mathrm{xm}}}\right)\\ &+2\cos^3\theta_{\mathrm{xm}}\Bigg)\Bigg/\left(2\sqrt{\lambda^2-\cos^2\theta_{\mathrm{xm}}}\left(\sin\theta_{\mathrm{xm}}\sqrt{\lambda^2-\cos^2\theta_{\mathrm{xm}}}+\sin^2\theta_{\mathrm{xm}}-\cos^2\theta_{\mathrm{xm}}+\lambda^2\right)\right) \end{aligned} \tag{38}$$

Equation (18c) is of the form:

$$2C_1 - \frac{C_2\,(\lambda^2-2)}{\sqrt{\lambda^2-1}} - K_0 = 0 \tag{39}$$

Substituting for C_1 from Eq. (36) into Eq. (39) leads to:

$$2\gamma_1 K_1 + \gamma_3 C_2 - K_0 = 0, \text{ where } \gamma_3 = 2\gamma_2 - \frac{\lambda^2-2}{\sqrt{\lambda^2-1}} \tag{40}$$

Substituting the expression of C_2 from Eq. (13) into Eq. (40), one obtains a quadratic equation in b as: $\rho g \gamma_3(\lambda+1)b^2 + Mg\gamma_3 b + 2\gamma_1 K_1 - K_0 = 0$. Considering $b > 0$, this equation provides a unique solution to b in terms of λ as follows:

$$b = \frac{\sqrt{\gamma_3^2 g^2 M^2 - 4\gamma_3 g(\lambda+1)\rho(2\gamma_1 K_1 - K_0)} - \gamma_3 gM}{2\gamma_3 g(\lambda+1)\rho} \tag{41}$$

Using this expression of b, it is possible to obtain C_2 (from Eq. (13)), and then C_1 in terms of λ. Further, from the definition of C_1 (see Eq. (18b)), the spring constant k can be found as: $k = \frac{C_1+2Mgd}{2b^2}$. The inequality in Eq. (18d) provides:

$$2C_1 - \frac{C_2\,(\lambda^2-2)}{\sqrt{\lambda^2-1}} + \frac{2bF_{\max}}{\sqrt{\lambda^2-1}} \geq 0 \tag{42}$$

Using Eq. (39), the above inequality can be simplified to:

$$K_0 + \frac{2bF_{\max}}{\sqrt{\lambda^2-1}} \geq 0 \tag{43}$$

Since both the terms on the left hand side of the above inequality are positive, it follows that the inequality would be satisfied by default without imposing any additional conditions.

Thus, the optimization problem for the design of the X-joint is posed as follows:

$$\begin{aligned} \underset{\lambda}{\text{Minimize}} \quad & F_{\max}(\lambda) = \frac{C_2\lambda^4 \sin\theta_{\text{xm}} \tan^2\theta_{\text{xm}} + K_1 \tan\theta_{\text{xm}}\,(\lambda^2 - \cos^2\theta_{\text{xm}})^{3/2}}{b\cos\theta_{\text{xm}}\left((\lambda^2-\cos^2\theta_{\text{xm}})^{3/2} - \sin^3\theta_{\text{xm}}\right)} \\ \text{subject to} \quad & k \in [0, 2000], \\ & b \in [0.05, 0.2], \\ & \lambda \in]1, 5], \end{aligned} \tag{44}$$

where λ is the only design variable in this problem ($\lambda = \frac{l}{b}$). The bounds on k and b must be transferred to λ, to define the feasible design space for X-joint. However, due to the complicated functional relationship between variables, an equivalent set of algebraic conditions on λ could not be derived. Nevertheless, from a plot of b (resp. k) against λ, it is possible to identify the feasible regions visually, and then compute the corresponding limiting points numerically, to define the feasible design space.

As in the previous case, the first-order necessary condition for $F_{\max}$ to attain a minima is obtained from the condition: $\frac{\mathrm{d}F_{\max}}{\mathrm{d}\lambda} = 0$. The corresponding algebraic expression is found to be:

$$\frac{\mathrm{d}F_{\max}}{\mathrm{d}\lambda} = \frac{\lambda \tan^3\theta_{\mathrm{xm}} \left(C_2\lambda^2 \left((\lambda^2 - 4\cos^2\theta_{\mathrm{xm}})\sqrt{\lambda^2 - \cos^2\theta_{\mathrm{xm}}} - 4\sin^3\theta_{\mathrm{xm}} \right) + 3K_1 \sin\theta_{\mathrm{xm}} \cos\theta_{\mathrm{xm}} \sqrt{\lambda^2 - \cos^2\theta_{\mathrm{xm}}} \right)}{b\left((\lambda^2 - \cos^2\theta_{\mathrm{xm}})^{3/2} - \sin^3\theta_{\mathrm{xm}} \right)^2} + \frac{\lambda^4 \tan^3\theta_{\mathrm{xm}}}{b\left((\lambda^2 - \cos^2\theta_{\mathrm{xm}})^{3/2} - \sin^3\theta_{\mathrm{xm}} \right)} \frac{\mathrm{d}C_2}{\mathrm{d}\lambda}, \tag{45}$$

where

$$\frac{\mathrm{d}C_2}{\mathrm{d}\lambda} = -\frac{2K_1}{\gamma_3}\frac{\mathrm{d}\gamma_1}{\mathrm{d}\lambda} + -\frac{K_0 - 2\gamma_1 K_1}{\gamma_3^2}\frac{\mathrm{d}\gamma_3}{\mathrm{d}\lambda}, \text{ in which,} \tag{46}$$

$$\frac{\mathrm{d}\gamma_1}{\mathrm{d}\lambda} = \frac{2\gamma_1^2 \lambda \sin\theta_{\mathrm{xm}} \cos^2\theta_{\mathrm{xm}} \left(2\sin\theta_{\mathrm{xm}} \sqrt{\lambda^2 - \cos^2\theta_{\mathrm{xm}}} - \cos^2\theta_{\mathrm{xm}} + \lambda^2 \right)}{(\lambda^2 - \cos^2\theta_{\mathrm{xm}})^{5/2}} \tag{47}$$

$$\frac{\mathrm{d}\gamma_3}{\mathrm{d}\lambda} = \frac{\lambda^3 \sec^3\theta_{\mathrm{xm}} \left(2\sin\theta_{\mathrm{xm}} \sqrt{\lambda^2 - \cos^2\theta_{\mathrm{xm}}} + 3\cos^4\theta_{\mathrm{xm}} - 7\cos^2\theta_{\mathrm{xm}} + \lambda^2 + 3 \right)}{\sqrt{\lambda^2 - \cos^2\theta_{\mathrm{xm}}} \left(\sin\theta_{\mathrm{xm}} \sqrt{\lambda^2 - \cos^2\theta_{\mathrm{xm}}} + \sin^2\theta_{\mathrm{xm}} - \cos^2\theta_{\mathrm{xm}} + \lambda^2 \right)^2} - \frac{\lambda^3}{(\lambda^2 - 1)^{3/2}} \tag{48}$$

Due to the complexity of the associated expressions, it is very difficult to obtain the solutions to $\frac{\mathrm{d}F_{\max}}{\mathrm{d}\lambda} = 0$, analytically. However, it is possible to solve this equation numerically once the values of parameters in the problem are substituted. Solution to the said equation would provide the stationary points of $F_{\max}$. Firstly, it is essential to check if there are solution(s) that satisfy all the constraints specified in Eq. (44). Secondly, such solutions must be classified as a minimum or a maximum or an inflection point, through the second derivative test or by inspecting the plot of $F_{\max}$ against λ. In case several minima exist within the feasible design space, then the one that corresponds to the least value of $F_{\max}$ must be chosen. On the other hand, if no minima exists, then the solution to this problem must be at/near a boundary of the feasible design space, depending on whether the boundary point is included or not.

5 Conclusion

The static analysis of two antagonistically actuated joints with a point mass payload has been conducted in this study: the revolute (R) joint and the antiparallelogram (X) joint. An optimal design strategy has been proposed to minimize the actuation forces for a prescribed wrench-feasible workspace (WFW) with a prescribed stiffness at rest and at the WFW bounds. It is possible to use the proposed strategy to design the R-joint and X-joint for the same WFW and compare the optimal designs on the basis of actuation forces and stiffness.

Acknowledgement This work was conducted with the support of the French National Research Agency (AVINECK Project ANR-16-CE33-0025).